



OPEN ACCESS

EDITED BY

Abhilash Kumar Tripathi,
Fujifilm Diosynth Biotechnologies Texas LLC,
United States

REVIEWED BY

Seha Kamil Saygili,
Istanbul University-Cerrahpasa, Cerrahpasa
Faculty of Medicine, Department of Pediatric
Nephrology, Türkiye
Jeremiah Abok,
University of New Mexico, United States

*CORRESPONDENCE

Paola Krall,
✉ paola.krall@uchile.cl

RECEIVED 15 January 2025

ACCEPTED 06 March 2025

PUBLISHED 23 April 2025

CITATION

Gajardo M, Guerrero JL, Poblete B, Bayyad E,
Castro I, Maturana J, Tobar J, Faúndes V and
Krall P (2025) Systematic use of protein free
energy changes for classifying variants of
uncertain significance: the case of IFT140 in
Mainzer-Saldino Syndrome.
Front. Mol. Biosci. 12:1561380.
doi: 10.3389/fmolb.2025.1561380

COPYRIGHT

© 2025 Gajardo, Guerrero, Poblete, Bayyad,
Castro, Maturana, Tobar, Faúndes and Krall.
This is an open-access article distributed
under the terms of the [Creative Commons
Attribution License \(CC BY\)](#). The use,
distribution or reproduction in other forums is
permitted, provided the original author(s) and
the copyright owner(s) are credited and that
the original publication in this journal is cited,
in accordance with accepted academic
practice. No use, distribution or reproduction
is permitted which does not comply with
these terms.

Systematic use of protein free energy changes for classifying variants of uncertain significance: the case of IFT140 in Mainzer-Saldino Syndrome

Macarena Gajardo¹, José Luis Guerrero², Bárbara Poblete³,
Esperanza Bayyad³, Ignacio Castro⁴, Jorge Maturana⁴,
Jaime Tobar⁵, Víctor Faúndes⁶ and Paola Krall^{1,7,8*}

¹Facultad de Medicina, Universidad de Chile, Santiago, Chile, ²Servicio de Nefrología, Hospital Luis Calvo Mackenna, Santiago, Chile, ³Escuela de Tecnología Médica, Facultad de Medicina, Universidad Austral de Chile, Valdivia, Chile, ⁴Instituto de Informática, Facultad de Ciencias e Ingeniería, Universidad Austral de Chile, Valdivia, Chile, ⁵Servicio de Pediatría, Hospital de Arica, Arica, Chile, ⁶Laboratorio de Genética y Enfermedades Metabólicas, Instituto de Nutrición y Tecnología de los Alimentos, Universidad de Chile, Santiago, Chile, ⁷Laboratorio de Nefrología, Facultad de Medicina, Universidad Austral de Chile, Valdivia, Chile, ⁸Centro de Investigación Clínica Avanzada (CICA)-Hospital Luis Calvo Mackenna, Santiago, Chile

Introduction: Advanced genetic strategies have transformed our understanding of the genetic basis and diagnosis of many phenotypes, including rare diseases. However, missense variants (MVs) are frequently identified and often classified as variants of uncertain significance (VUS). Although changes in protein free energy ($\Delta\Delta G$) were recently proposed as a tool for VUS classification, no objective cut-offs exist to distinguish between benign and pathogenic variants.

Methods: We utilized the computational tool mCSM to calculate $\Delta\Delta G$ and predict the impact of MVs on protein stability. Specifically, we systematically analyzed the $\Delta\Delta G$ of MVs in IFT140 to identify those potentially pathogenic and associated with Mainzer-Saldino syndrome (MSS). To this end, we evaluated $\Delta\Delta G$ in IFT140 MVs sourced from ClinVar, gnomAD, and MSS patients, aiming to resolve the diagnosis of MSS in a child with a novel homozygous IFT140 variant, initially reported as a VUS.

Results: IFT140 MVs from MSS patients showed lower $\Delta\Delta G$ values than those reported in gnomAD individuals (-1.389 vs. -0.681 kcal/mol; $p = 0.0031$). A ROC curve demonstrated strong discriminative ability ($AUC = 0.8488$; $p = 0.0002$), and a $\Delta\Delta G$ cut-off of -1.3 kcal/mol achieving 50% sensibility and 90% specificity. The analysis of ClinVar IFT140 variants classified as VUS, showed that 75/323 (23%) presented $\Delta\Delta G$ values below the cut-off. In the child clinically suspicious of MSS, this cut-off allowed the reclassification of the VUS (IFT140:p.W80C; $\Delta\Delta G = -1.745$ kcal/mol) as likely pathogenic, which confirmed the diagnosis molecularly.

Conclusion: Our findings demonstrate that $\Delta\Delta G$ analysis can effectively distinguish potentially pathogenic variants in IFT140, enabling confirmation

of MSS. The established cut-off of -1.3 kcal/mol showed strong discriminative power, aiding in the reclassification of VUS identified in IFT140. This approach highlights the utility of protein stability predictions in resolving diagnostic uncertainty in rare diseases.

KEYWORDS

missense variant, bioinformatics, free energy changes, Mainzer-Saldino Syndrome, ciliopathy, IFT140

Introduction

Advanced genetic strategies have transformed our understanding of the basis and diagnosis of many diseases. Protein-truncating variants (PTV) are usually considered pathogenic due to their strong functional effects, with few exceptions. However, missense variants (MV) are more frequent than PTV and often classified as variants of uncertain significance (VUS) due to limited population frequency data and functional evidence, underscoring the need for improved methods of resolution (Richards et al., 2015), (Appelbaum et al., 2022).

Short-rib thoracic dysplasia 9 (SRTD9, OMIM#266920), or Mainzer-Saldino Syndrome (MSS), is an extremely rare ciliopathy affecting fewer than 1 in 1,000,000 individuals. MSS is characterized by chronic kidney disease (CKD), progressive vision impairment, with distinctive skeletal features such as cone-shaped epiphyses (Geoffroy et al., 2018). Around 20 MSS cases have been reported, involving homozygous or compound heterozygous variants in the Intraflagellar Transport 140 (*IFT140*) gene. *IFT140* contains multiple WD40 repeat (WD) and tetratricopeptide-repeat (TPR) domains that enable the protein to interact with others to form complex structures, facilitating the transport of proteins along the cilia. Accurate interpretation of *IFT140* variants is essential for MSS diagnosis, guiding personalized treatment, avoiding unnecessary interventions, informing prognosis, and identifying at-risk family members (Walsh et al., 2024). The identification of novel MVs in *IFT140* has a high likelihood of being classified as VUS, delaying diagnosis and limiting their clinical utility (Chen et al., 2023).

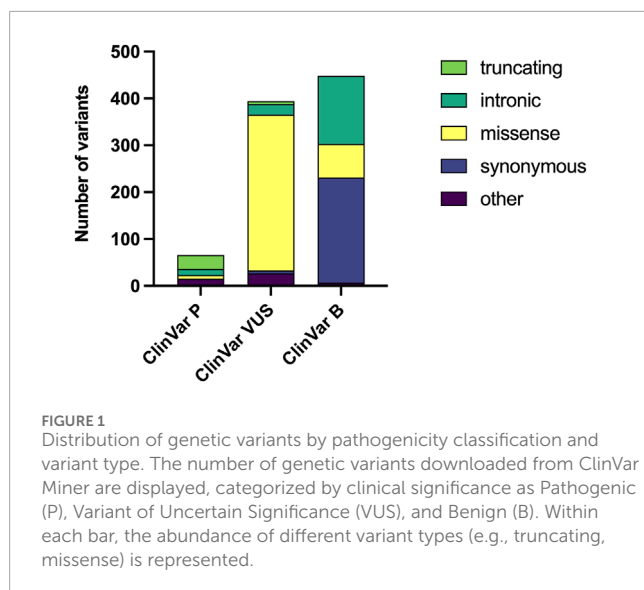
Several methods have been developed to enable VUS reclassification. These include population allele frequencies, functional assays, and machine learning models, with structural models specifically providing insights into the underlying molecular mechanisms. Gibbs free energy (ΔG) is a thermodynamic measure used to quantify protein stability, based on the principle that structures tend to adopt more negative energy states. If the difference between the folded and native forms of a protein results in a more negative value, the process occurs spontaneously. In this context, the change in Gibbs free energy ($\Delta\Delta G$) evaluates the difference between the Gibbs free energies of a wild-type and a mutant protein. A negative $\Delta\Delta G$ value indicates that the mutant protein is destabilizing (Sapozhnikov et al., 2023). Recently, the Association for Clinical Genomic Science (ACGS 2024) recommended the use of $\Delta\Delta G$ caused by MVs for their classification, based on a successful clinical experience (Caswell et al., 2022), (ACGS, 2024). However, the proposed $\Delta\Delta G$ cut-offs were subjectively determined as they did not consider the full spectrum of $\Delta\Delta G$ seen in both benign and pathogenic MVs (Caswell et al., 2022).

The mutation Cutoff Scanning Matrix (mCSM) was introduced in 2014 to predict MVs effects by assessing protein structure changes and stability using $\Delta\Delta G$ (Pires et al., 2014). It offers a computationally efficient, easy-to-use and well-validated approach with optimal correlation to experimental $\Delta\Delta G$ data. When analyzing amino acid substitutions in different human diseases, mCSM predicted a higher proportion of variants as destabilizing and demonstrated better predictive power compared to other structure-based tools (Choudhury et al., 2022). Herein, we aimed to systematically establish a $\Delta\Delta G$ cut-off for *IFT140* MVs using mCSM, which helped to confirm the molecular diagnosis of MSS in a child with a novel homozygous *IFT140* variant, initially classified as VUS.

Materials and methods

First, we aimed to compare the $\Delta\Delta G$ seen in benign versus pathogenic *IFT140* MVs to establish a cut-off that allowed us to distinguish between these two groups and reclassify VUS deposited in ClinVar. For this purpose, we downloaded *IFT140* variants from ClinVar Miner (version 06-30-2024) with their ACMG classifications: P and LP were combined into the pathogenic (ClinVar-P) group, B and LB were combined into the benign (ClinVar-B) group, and VUS (ClinVar-VUS) were kept as a separate group (Henrie et al., 2018). Minor allele frequency (MAF) was assessed in each group using the gnomAD v4.1 database. Homozygous *IFT140* MVs were obtained from gnomAD, focusing on LB/B classifications according to ClinVar and assumed as controls (Chen et al., 2024). Homozygous or compound heterozygous *IFT140* MVs associated with MSS phenotype were collected and considered as cases (Geoffroy et al., 2018), (Patel et al., 2023), (Perrault et al., 2012), (Yeh et al., 2022), (Soyaltın et al., 2018), (Schmidts et al., 2013), (Oud et al., 2018). PTVs or synonymous *IFT140* variants were excluded. The PDB file for IFT140 (8BBG, 3.50 Å, chain B, positions 1–1462) was downloaded from UniProt and used to calculate $\Delta\Delta G$ for each MV using mCSM (<https://biosig.lab.uq.edu.au/mcsm/>) (Pires et al., 2014). Mean $\Delta\Delta G$ values from gnomAD and MSS variants were compared using Mann-Whitney U test, and Receiver Operating Characteristic (ROC) curve was constructed to define a $\Delta\Delta G$ cut-off. In addition, the distribution of variants in *IFT140* was evaluated, focusing on the 7 WD and 9 TPR domains according to the information available on UniProt. We made a statistical analysis of the position within and outside these domains comparing gnomAD and MSS patients. Chi square test was considered to determine statistical significances of these distributions.

Second, we aimed to reclassify a novel homozygous *IFT140* MV seen in a patient with a phenotype compatible with MSS and



considering the obtained cut-off, and to study the relevance of the affected residue for the syndrome. For these purposes, detailed clinical history and exome data were collected and informed consent was obtained from parents. The identified *IFT140* variant and all possible residue changes underwent systematic $\Delta\Delta G$ analysis using mCSM, to compare those values with the cut-off. The study was revised and approved by the Ethics Committee from the Servicio de Salud Los Ríos.

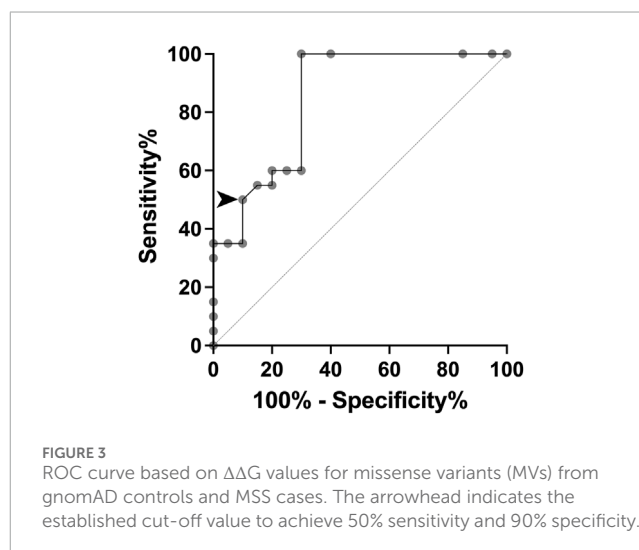
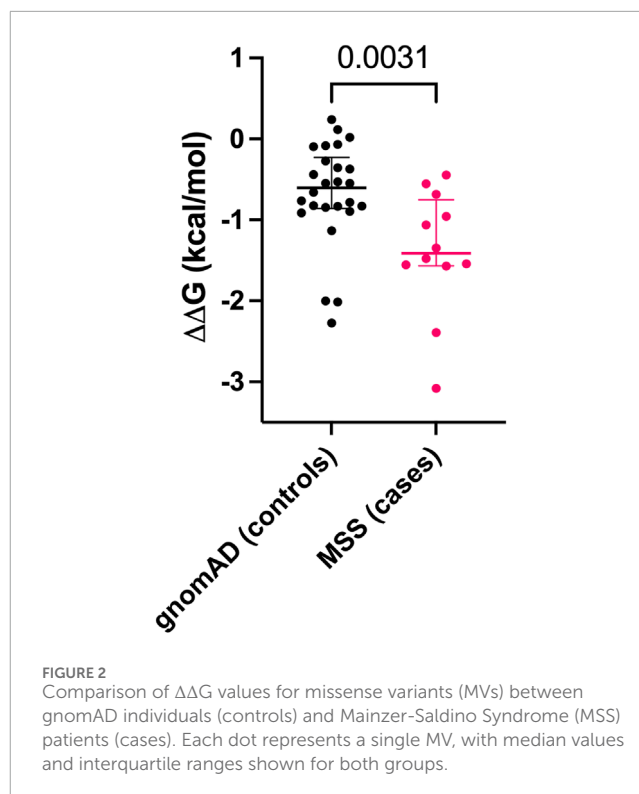
Results

We obtained 908 genetic changes registered in ClinVar as variants compromising *IFT140*. These changes included 412 (45.4%) MVs, 230 (25.3%) synonymous variants, 181 (19.9%) intronic variants with different possible impacts, 49 (5.4%) rearrangements that involved *IFT140*, and only 36 (4.0%) PTVs.

When considering their classification, 66 variants were ClinVar-P, 394 variants were considered ClinVar-VUS, and 448 variants were ClinVar-B (Figure 1). In the ClinVar-P group, 43 (65.2%) variants were PTVs. MVs represented 84.3% of all variants in ClinVar-VUS, while they were found in 16.1% and 12.1% of the ClinVar-B and ClinVar-P groups, respectively.

The gnomAD database showed the MAF for 196 of all the MVs in the different ClinVar groups. The average MAFs in the ClinVar-P, ClinVar-VUS and ClinVar-B groups were 0.475, 0.250 and 38.76 per 10,000 individuals, respectively. Of note, 29 (49.1%) out of 59 MVs in the ClinVar-B group had a MAF of less than 1 in 10,000, while in the ClinVar-VUS group, this characteristic was observed in 130 out of 133 MVs.

We calculated $\Delta\Delta G$ for gnomAD individuals with homozygous *IFT140* MVs ($n = 26$) and for MSS patients (3 homozygous and 9 heterozygous MVs). The mean $\Delta\Delta G$ for gnomAD MVs was -0.681 kcal/mol (95%CI: -0.937 to -0.426) and for MSS MVs it was -1.389 kcal/mol (95%CI: -1.872 to -0.907). The difference in $\Delta\Delta G$ values between gnomAD and MSS *IFT140* MVs was significant ($U = 64$, $p = 0.0031$) (Figure 2).



By using our $\Delta\Delta G$ data in gnomAD individuals and MSS patients, we constructed the ROC curve and obtained an AUC of 0.8488 ($p = 0.0002$), indicating an optimal discriminative ability to identify likely pathogenic MVs. The cut-off point was established at $\Delta\Delta G -1.3$ kcal/mol, yielding a sensitivity of 50% and a specificity of 90% (Figure 3). For ClinVar groups, the average $\Delta\Delta G$ values were -1.432 kcal/mol (95%CI: -2.074 to -0.789), -0.798 kcal/mol (95%CI: -0.878 to -0.717), and -0.796 kcal/mol (95%CI: -0.953 to -0.640), for *IFT140* MVs classified as pathogenic, VUS, or benign, respectively. Of note, in the ClinVar-VUS group, 75/323 MVs had $\Delta\Delta G$ values below -1.3 kcal/mol (Supplementary Figure S1).

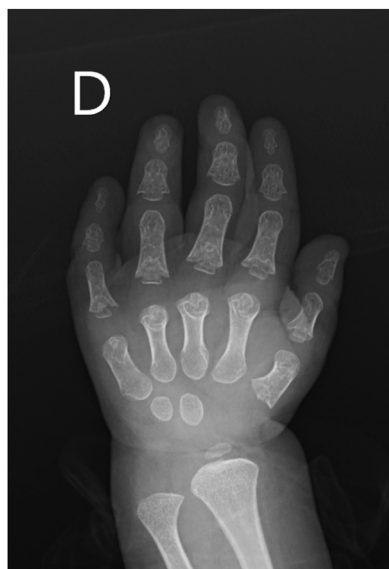


FIGURE 4
X-ray image of the right hand from the pediatric patient suspected of having Mainzer-Saldino Syndrome (MSS). The image reveals characteristic skeletal abnormalities associated with MSS (cone-shaped epiphyses).

The analysis from gnomAD individuals and MSS patients regarding their MV positions within and outside WD and TPR domains showed that 7 out of 26 variants (27%) reported in gnomAD homozygous individuals and 5 out of 9 variants (56%) identified in MSS patients were in these domains. However, this difference did not reach statistical significance ($p = 0.1255$).

A novel homozygous *IFT140* variant was discovered in a 1.5-year-old girl who was evaluated for CKD stage 4 with small kidneys without cystic pattern, hepatic fibrosis, neurological developmental delay, and unilateral moderate sensorineural hearing loss. The array comparative genomic hybridization was normal, *PKD1* analysis by long-range PCR sequencing was negative, but exome sequencing identified the *IFT140* c.240G>T (p.W80C) homozygous MV categorized as VUS. This variant was inherited from both heterozygous parents aged 34 and 43 years, who underwent abdominal ultrasounds, with no relevant findings observed, particularly in the kidney structures (Dordoni et al., 2024). Subsequent evaluations in the patient revealed retinal dystrophy, and phalangeal cone-shaped epiphyses in both hands (Figure 4), confirming the clinical diagnosis of MSS. The $\Delta\Delta G$ value for *IFT140*:p.W80C was -1.745 kcal/mol, and further systematic evaluation of the W80 residue indicated that all possible amino acid substitutions were destabilizing (Table 1).

Discussion

Rare diseases are a heterogeneous group of conditions with an emerging global impact, a population prevalence of 3.5%–5.9% and with a genetic origin in almost 80% (Nguengang et al., 2020). The rate of VUS in genes associated with rare diseases is 41.5%, and MVs

represent the largest proportion of them (86.6%) (Chen et al., 2023). Half of the *IFT140* benign MVs had a $MAF < 1/10,000$ suggesting that rarity of a variant is not a reliable indicator of pathogenicity and reinforcing the need of additional methods for reanalysis.

In recent years, increasing interest in predicting the pathogenicity of MVs VUS using structure-based algorithms has emerged (Pan and Theesfeld, 2024). One such approach involves calculating the $\Delta\Delta G$ between the wild-type and variant residues; however, establishing a valid cut-off value is essential (Pires et al., 2014), (David and Sternberg, 2023). Recent studies have demonstrated that $\Delta\Delta G$ is a useful tool for evaluating other MVs in genes such as transcription factor *FOXD2* and *TBC1D31* which are now implicated in syndromic congenital anomalies of the kidney and urinary tract (Riedhammer et al., 2024; Saygılı et al., 2023), as well as *NUP85*, associated with steroid-resistant nephrotic syndrome (Şükür et al., 2025). In the field of protein stability, various computational tools aid in the assessment of MVs, including mCSM, Dynamut2 (Rodrigues et al., 2021), FoldX (Schymkowitz et al., 2005) and PremPS (Chen et al., 2020), among others. These tools evaluated stability, folding and dynamics of proteins. Additionally, molecular dynamics simulations offer valuable insights into atomic movements within a protein by modeling interatomic interactions (Hollingsworth and Dror, 2018).

The $\Delta\Delta G$ in *IFT140* MVs revealed significant differences between benign (gnomAD individuals) and pathogenic (MSS patients) variants. We established a cut-off value of -1.3 kcal/mol with an optimal sensitivity and specificity for *IFT140* MVs. When analyzing the totality of MVs in the ClinVar-VUS group, we identified that 23.2% had $\Delta\Delta G$ values below the cut-off value, suggesting that these might be re-classified as likely pathogenic.

The novel variant *IFT140*:p.W80C found in our female patient, initially classified as VUS, is a good example of the impact of our work. The child met all clinical features to be diagnosed with MSS (Soyaltın et al., 2018), and the $\Delta\Delta G$ value of -1.745 kcal/mol for p.W80C, below our calculated cut-off, confirms the deleteriousness of this variant. Additionally, the destabilizing values of all possible substitutions at this position indicate its intolerance to amino acid changes, which allowed us to reclassify the p.W80C as likely pathogenic, following ACGS 2024 recommendations (ACGS, 2024).

Our study has limitations in different aspects. Firstly, few patients with MSS and gnomAD *IFT140* homozygous individuals have been reported, which decreases the sensibility of our findings. However, this is the first study to our knowledge that systematically evaluates a $\Delta\Delta G$ cut-off value in patients with *IFT140* VUS, which has the potential to be used for the evaluation of other similar patients. Further calculations of $\Delta\Delta G$ cut-offs for other monogenic diseases are required to implement the recent ACGS 2024 recommendations of structural damage for MVs classification (ACGS, 2024).

Bioinformatic tools that evaluate $\Delta\Delta G$ have several limitations, many of which depend on structural data availability. Most require a high-resolution 3D protein structure, typically from Protein Data Bank (PDB). If the variant of interest is in a flexible or disordered region that is not well-captured in the structure, predictions can be unreliable. When no structure is available, these tools must rely on homology modeling, which introduces additional errors compared to crystal structures. Additionally, environmental effects are often poorly accounted for in these tools. Factors

TABLE 1 $\Delta\Delta G$ values obtained for all possible substitutions of the IFT140 W80 residue with the pdb file downloaded with the identifier 8BBG. The substitution W80C seen in the child has been highlighted in bold.

Index	Wild type residue	Position	Mutant residue	Predicted $\Delta\Delta G$	Outcome
1	W	80	A	−3.989	Highly Destabilizing
2	W	80	V	−3.545	Highly Destabilizing
3	W	80	L	−3.277	Highly Destabilizing
4	W	80	G	−4.16	Highly Destabilizing
5	W	80	S	−3.146	Highly Destabilizing
6	W	80	T	−2.99	Highly Destabilizing
7	W	80	Q	−2.936	Highly Destabilizing
8	W	80	E	−3.537	Highly Destabilizing
9	W	80	C	−1.745	Destabilizing
10	W	80	R	−1.994	Destabilizing
11	W	80	P	−3.545	Highly Destabilizing
12	W	80	D	−3.632	Highly Destabilizing
13	W	80	F	−2.661	Highly Destabilizing
14	W	80	I	−3.277	Highly Destabilizing
15	W	80	H	−2.97	Highly Destabilizing
16	W	80	N	−2.932	Highly Destabilizing
17	W	80	M	−2.535	Highly Destabilizing
18	W	80	Y	−2.418	Highly Destabilizing
19	W	80	K	−2.516	Highly Destabilizing

such as solvent interactions, post-translational modifications, *in vivo* physiological conditions, and protein-protein interactions are either oversimplified or completely ignored. This is particularly problematic when multiple pathogenic mechanisms coexist. Finally, $\Delta\Delta G$ prediction tools can yield conflicting results, as they rely on different algorithms and training datasets. To improve reliability, it might be reasonable to use multiple tools and compare their outputs.

By 2030, VUS in coding regions are expected to be resolved through several advancements, including refinements in variant classification standards, improved performance of computational variant effect predictors, the establishment of large-scale $\Delta\Delta G$ datasets, the development of hybrid *in silico* and experimental approaches, and enhanced data-sharing efforts that maximize the information gained from each newly sequenced individual and interpreted variant (Fowler and Rehm, 2024). Additionally, machine learning approaches will play a key role by integrating large-scale genomic, functional, and clinical data, improving predictive accuracy, and identifying complex patterns that traditional methods might overlook (Quazi, 2022; Khalifa and Albadowy, 2024).

In conclusion, the analysis of $\Delta\Delta G$ can aid in the evaluation of *IFT140* MVs for diagnostic purposes. The appropriate approach should include the assessment of clinical findings, the evaluation of genetic variants using meta-predictors or other assays, with $\Delta\Delta G$ serving as one of the components of the comprehensive strategy in patients suspected to have MSS or other rare diseases. Future advancements in variant classification standards, computational predictors, multiplexed assays, and machine learning approaches will further enhance the interpretation of $\Delta\Delta G$ and its role in variant assessment, especially those of uncertain significance.

Data availability statement

The datasets presented in this study can be found in online repositories. The names of the repository/repositories and accession number(s) can be found below: Figshare, doi: 10.6084/m9.figshare.28199999, https://figshare.com/articles/dataset/Kidney_Panel_Variants/28199999?file=51653081.

Ethics statement

The studies involving humans were approved by Comité Ético-Científico, Servicio de Salud Valdivia-Los Ríos. The studies were conducted in accordance with the local legislation and institutional requirements. Written informed consent for participation in this study was provided by the participant's legal guardians/next of kin. Written informed consent was obtained from the individual(s) for the publication of any potentially identifiable images or data included in this article.

Author contributions

MG: Data curation, Formal Analysis, Investigation, Methodology, Writing—original draft. JG: Data curation, Writing—review and editing. BP: Data curation, Investigation, Writing—review and editing. EB: Data curation, Investigation, Writing—review and editing. IC: Investigation, Software, Writing—review and editing. JM: Investigation, Software, Writing—review and editing. JT: Data curation, Investigation, Writing—review and editing. VF: Conceptualization, Data curation, Funding acquisition, Investigation, Methodology, Supervision, Writing—original draft, Writing—review and editing. PK: Conceptualization, Formal Analysis, Funding acquisition, Methodology, Project administration, Supervision, Validation, Writing—original draft, Writing—review and editing.

Funding

The author(s) declare that financial support was received for the research, authorship, and/or publication of this article. Partial funding was obtained from the grant FIC22-13 (Fondo de Innovación a la Competitividad, Gobierno Regional Los Ríos), FONDECYT de Iniciación #11240332, FONDECYT Regular #1250968 and Núcleo RinHOS.

References

- ACGS (2024). ACGS best practice guidelines for variant classification in rare disease. Available online at: <https://www.acgs.uk.com/media/12533/uk-practice-guidelines-for-variant-classification-v12-2024.pdf>.
- Appelbaum, P. S., Burke, W., Parens, E., Zeevi, D. A., Arbour, L., Garrison, N. A., et al. (2022). Is there a way to reduce the inequity in variant interpretation on the basis of ancestry? *Am. J. Hum. Genet.* 109 (6), 981–988. doi:10.1016/j.ajhg.2022.04.012
- Caswell, R. C., Gunning, A. C., Owens, M. M., Ellard, S., and Wright, C. F. (2022). Assessing the clinical utility of protein structural analysis in genomic variant classification: experiences from a diagnostic laboratory. *Genome Med.* 14 (1), 77. doi:10.1186/s13073-022-01082-2
- Chen, E., Facio, F. M., Aradhya, K. W., Rojahn, S., Hatchell, K. E., Aguilar, S., et al. (2023). Rates and classification of variants of uncertain significance in hereditary disease genetic testing. *JAMA Netw. Open* 6 (10), e2339571. doi:10.1001/jamanetworkopen.2023.39571
- Chen, S., Francioli, L. C., Goodrich, J. K., Collins, R. L., Kanai, M., Wang, Q., et al. (2024). A genomic mutational constraint map using variation in 76,156 human genomes. *Nature* 625, 92–100. doi:10.1038/s41586-023-06045-0
- Chen, Y., Lu, H., Zhang, N., Zhu, Z., Wang, S., and Li, M. (2020). PremPS: predicting the impact of missense mutations on protein stability. *PLoS Comput. Biol.* 16 (12), e1008543. doi:10.1371/journal.pcbi.1008543
- Choudhury, A., Mohammad, T., Anjum, F., Shafie, A., Singh, I. K., Abdullaev, B., et al. (2022). Comparative analysis of web-based programs for single amino acid substitutions in proteins. *PLoS One* 17 (5), e0267084. doi:10.1371/journal.pone.0267084
- David, A., and Sternberg, M. J. E. (2023). Protein structure-based evaluation of missense variants: resources, challenges and future directions. *Curr. Opin. Struct. Biol.* 80, 102600. doi:10.1016/j.sbi.2023.102600
- Dordoni, C., Zeni, L., Toso, D., Mazza, C., Mescia, F., Cortinovis, R., et al. (2024). Monoallelic pathogenic IFT140 variants are a common cause of autosomal dominant polycystic kidney diseasespectrum phenotype *Clin. Kidney J.* 17 (2), sfac026.
- Fowler, D. M., and Rehm, H. L. (2024). Will variants of uncertain significance still exist in 2030? *Am. J. Hum. Genet.* 111 (1), 5–10. doi:10.1016/j.ajhg.2023.11.005
- Geoffroy, V., Stoetzel, C., Scheidecker, S., Schaefer, E., Perrault, I., Bär, S., et al. (2018). Whole-genome sequencing in patients with ciliopathies uncovers a novel recurrent tandem duplication in IFT140. *Hum. Mutat.* 39 (8), 983–992. doi:10.1002/humu.23559
- Henrie, A., Hemphill, S. E., Ruiz-Schultz, N., Cushman, B., DiStefano, M. T., Azzariti, D., et al. (2018). ClinVar Miner: demonstrating utility of a Web-based tool for viewing and filtering ClinVar data. *Hum. Mutat.* 39 (8), 1051–1060. doi:10.1002/humu.23555
- Hollingsworth, S. A., and Dror, R. O. (2018). Molecular dynamics simulation for all. *Neuron* 99 (6), 1129–1143. doi:10.1016/j.neuron.2018.08.011

Acknowledgments

We gratefully acknowledge the invaluable support and expertise provided by the Servicio de Genética at Hospital Luis Calvo Mackenna, whose dedication and assistance were crucial in the successful completion of the genetic analysis of the patient.

Conflict of interest

The authors declare that the research was conducted in the absence of any commercial or financial relationships that could be construed as a potential conflict of interest.

Generative AI statement

The authors declare that Gen AI was used in the creation of this manuscript. Grammarly was used to identify and correct grammar, spelling, punctuation errors, and improve tone, and clarity.

Publisher's note

All claims expressed in this article are solely those of the authors and do not necessarily represent those of their affiliated organizations, or those of the publisher, the editors and the reviewers. Any product that may be evaluated in this article, or claim that may be made by its manufacturer, is not guaranteed or endorsed by the publisher.

Supplementary material

The Supplementary Material for this article can be found online at: <https://www.frontiersin.org/articles/10.3389/fmolb.2025.1561380/full#supplementary-material>

- Khalifa, M., and Albadawy, M. (2024). Artificial intelligence for clinical prediction: exploring key domains and essential functions. *Comput. Meth. Prog. Bio.* 5, 100148. doi:10.1016/j.cmpbup.2024.100148
- Nguengang, S., Lambert, D. M., Olry, A., Rodwell, C., Gueydan, C., Lanneau, V., et al. (2020). Estimating cumulative point prevalence of rare diseases: analysis of the Orphanet database. *Eur. J. Hum. Genet.* 28 (2), 165–173. doi:10.1038/s41431-019-0508-0
- Oud, M. M., Latour, B. L., Bakey, Z., Letteboer, S. J., Lugtenberg, D., Wu, K. M., et al. (2018). Cellular ciliary phenotyping indicates pathogenicity of novel variants in IFT140 and confirms a Mainzer-Saldino syndrome diagnosis. *Cilia* 7, 1. doi:10.1186/s13630-018-0055-2
- Pan, Z., and Theesfeld, C. L. (2024). Deciphering missense coding variants with AlphaMissense. *Kidney Int.* 106 (2), 175–178. doi:10.1016/j.kint.2024.02.022
- Patel, S. H., Bakhsh, S., Conboy, E., and Hajrasouliha, A. R. (2023). Case of ift140-associated mainzer saldino syndrome. *Ophthalmic Genet.* 44 (2), 208–210. doi:10.1080/13816810.2022.2113545
- Perrault, I., Saunier, S., Hancin, S., Filhol, E., Bizet, A. A., Collins, F., et al. (2012). Mainzer-Saldino syndrome is a ciliopathy caused by IFT140 mutations. *Am. J. Hum. Genet.* 90 (5), 864–870. doi:10.1016/j.ajhg.2012.03.006
- Pires, D. E., Ascher, D. B., and Blundell, T. L. (2014). mCSM: predicting the effects of mutations in proteins using graph-based signatures. *Bioinformatics* 30 (3), 335–342. doi:10.1093/bioinformatics/btt691
- Quazi, S. (2022). Artificial intelligence and machine learning in precision and genomic medicine. *Med. Oncol.* 39, 120. doi:10.1007/s12032-022-01711-1
- Richards, S., Aziz, N., Bale, S., Bick, D., Das, S., Gastier-Foster, J., et al. (2015). Standards and guidelines for the interpretation of sequence variants: a joint consensus recommendation of the American college of medical genetics and genomics and the association for molecular pathology. *Genet. Med.* 17 (5), 405–424. doi:10.1038/gim.2015.30
- Riedhammer, K. M., Nguyen, T. T., Koşukcu, C., Calzada-Wack, J., Li, Y., Assia Batzir, N., et al. (2024). Implication of transcription factor FOXD2 dysfunction in syndromic congenital anomalies of the kidney and urinary tract (CAKUT). *Kidney Int.* 105 (4), 844–864. doi:10.1016/j.kint.2023.11.032
- Rodrigues, C. H. M., Pires, D. E. V., and Ascher, D. B. (2021). DynaMut2: assessing changes in stability and flexibility upon single and multiple point missense mutations. *Protein Sci.* 30 (1), 60–69. doi:10.1002/pro.3942
- Sapozhnikov, Y., Patel, J. S., Ytreberg, F. M., and Miller, C. R. (2023). Statistical modeling to quantify the uncertainty of FoldX-predicted protein folding and binding stability. *BMC Bioinforma.* 24 (1), 426. doi:10.1186/s12859-023-05537-0
- Saygılı, S., Koşukcu, C., Baştuğ, T., Doğan, Ö. A., Yılmaz, E. K., Kalyoncu, A. U., et al. (2023). A novel homozygous missense variant in TBC1D31 in a consanguineous family with congenital anomalies of the kidney and urinary tract (CAKUT). *Clin. Genet.* 104 (6), 679–685. doi:10.1111/cge.14406
- Schmidts, M., Frank, V., Eisenberger, T., Turki, S., Bizet, A., Antony, D., et al. (2013). Combined NGS approaches identify mutations in the intraflagellar transport gene IFT140 in skeletal ciliopathies with early progressive kidney Disease. *Hum. Mutat.* 34 (5), 714–724. doi:10.1002/humu.22294
- Schymkowitz, J., Borg, J., Stricher, F., Nys, R., Rousseau, F., and Serrano, L. (2005). The FoldX web server: an online force field. *Nucleic Acids Res.* 33 (Web Server issue), W382–W388. doi:10.1093/nar/gki387
- Soyaltın, E., Kasap-Demir, B., Alparslan, C., Arslansoyu-Camlar, S., Perihan, K. O., Kırbyık, Ö., et al. (2018). Can a hand radiograph indicate a special diagnosis in a child with chronic kidney disease? Answers. *Pediatr. Nephrol.* 33 (5), 801–803. doi:10.1007/s00467-017-3742-0
- Şükür, E. D. K., Timucin, E., Baştuğ, T., and Ozaltın, F. (2025). A novel NUP85 variant expanding the phenotypic spectrum of NUP85-associated steroid-resistant nephrotic syndrome. *Clin. Genet.* doi:10.1111/cge.14703
- Walsh, N., Cooper, A., Dockery, A., and O'Byrne, J. J. (2024). Variant reclassification and clinical implications. *J. Med. Genet.* 61 (3), 207–211. doi:10.1136/jmg-2023-109488
- Yeh, T. C., Niu, D. M., Cheng, H. C., Chen, Y. R., Chen, L. Z., Tsui, S. P., et al. (2022). Novel mutation of IFT140 in an infant with Mainzer-Saldino syndrome presenting with retinal dystrophy. *Mol. Genet. Metab. Rep.* 33, 100937. doi:10.1016/j.ymgmr.2022.100937